JOURNAL OF MATERIALS SCIENCE 27 (1992) 3032–3035

Effect of scandium on the decomposition of aluminium–zinc alloys

J. DUTKIEWICZ
Institute for Metal Research, Polish Academy of Sciences, ul. Reymonta 25, 30-059 Krakow, Poland

A. M. ZAHRA, C. Y. ZAHRA
Centre de Thermodynamique et de Microcalorimétrie du CNRS, 26, rue du 141e RIA, 13003 Marseille, France

The effect of scandium on the hardness, structure and heat evolution of an aluminium–40% zinc alloy was investigated. It was found that contrary to its action in other aluminium-based alloys, scandium does not raise the maximum hardness during an ageing treatment. This may be explained by insufficient scandium redissolution at the rather low temperature necessary for achieving a solid solution of zinc in aluminium. Differential scanning calorimetry studies show a similar heat evolution in both alloys upon linear heating, starting with the reversion of modulated structures. An exothermal effect appears only in the scandium-bearing alloy due to increased heterogeneous precipitation of α'_r and β on Al_3Sc particles. Above 200 °C, the dissolution of the α'_r and β phases starts, followed by the monotectoid reaction.

1. Introduction

A small addition of scandium to aluminium–magnesium [1] or other aluminium alloys [2, 3] increases significantly hardness and yield stress during ageing. The additional effect of hardening during ageing is due to the precipitation of finely distributed, ordered Al_3Sc particles. The decomposition of aluminium–zinc alloys is also affected by small additions of a third element [4, 5] modifying, particularly in the presence of magnesium, the kinetics of β-Zn and of a α'_r transition phase formation. In the present work the influence of a small addition of scandium to an aluminium–40% zinc alloy was investigated with respect to structure changes, as well as hardness and heat evolution.

2. Experimental procedure

Alloys were cast from 99.99% pure elements. Their compositions are given in Table I, as determined by atomic emission spectrometry. Specimens were homogenized at 360 °C for 2 days in order to eliminate the dendritic segregation. Then they were annealed at 450 °C for 1 h and quenched into water at 20 °C.

Samples for differential scanning calorimetry (DSC) were investigated after various ageing times at room temperature (RT). A DuPont thermal analyser, model 990, was employed at two heating rates, 5 and 20 °C min^{-1}, between 0 and 400 °C. The experimental curves are presented in such a way as to permit a direct comparison of different peak areas and hence of enthalpy changes observed during heating. Structure changes were investigated using a Philips EM-400 electron microscope operating at 120 kV. Thin foils were obtained by jet disc electropolishing in an electrolyte containing 25% HNO_3 and 75% CH_3OH at − 30 °C. Hardness changes were measured during ageing using a Vickers tester.

3. Results and discussion

Fig. 1 shows hardness–ageing time curves at 100 °C for Alloys A and B. It can be seen that a maximum value appears around 140 HV and is slightly higher for Alloy A without scandium. Both alloys attain the maximum after about 1 h ageing. Alloys annealed at 150 °C display similar hardness curves with maxima of about 140 HV after 20 min ageing. Compared to the effect of copper [6] or magnesium [7], the influence of scandium on mechanical properties is insignificant. This may be attributed to the low scandium solubility at the applied homogenization temperature of 450 °C which limits the precipitation of finely distributed Al_3Sc particles during ageing. Temperatures above 500 °C are needed in order to increase the scandium content in binary aluminium–scandium solid solutions [8], but the solidus in the aluminium–40% zinc alloy is already reached at 500 °C.

Fig. 2 shows DSC curves of Alloys A and B quenched from 450 °C, aged 7 days at RT and heated to 400 °C at a rate of 5 °C min^{-1}. A comparison of these curves shows that both alloys exhibit, at first, endothermal effects and then only Alloy B displays an exothermal one. A strong endothermal peak merges above 270 °C with the preceding one and corresponds to the monotectoid reaction $\alpha + \beta \rightarrow \alpha + \alpha'$. This is of equal importance in both alloys, taking into account that precipitation during the DSC-scan in Alloy B

0022–2461

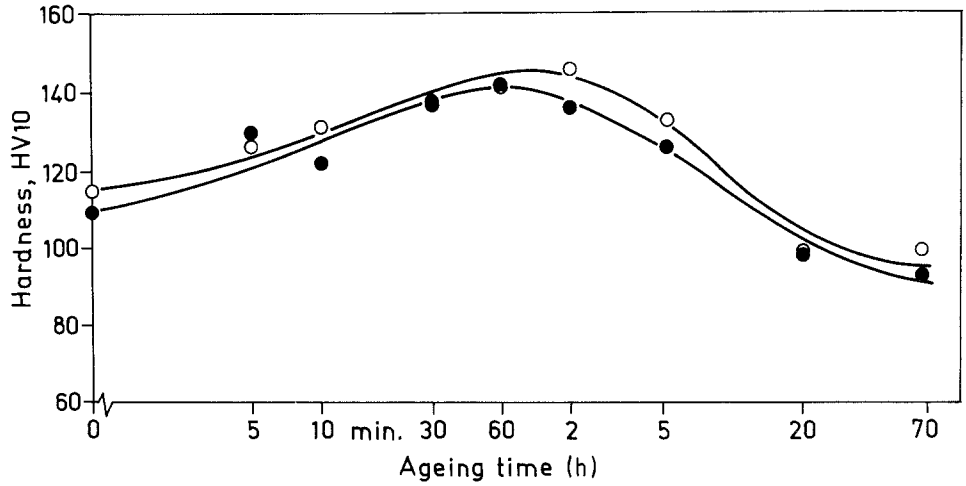

Figure 1 Hardness versus ageing time at 100 °C for Alloys (○) A and (●) B.

TABLE I Compositions of alloys investigated

Alloy	Composition (wt %)		
	Zn	Sc	Al
A	40.1	–	Bal.
B	39.56	0.15	Bal.

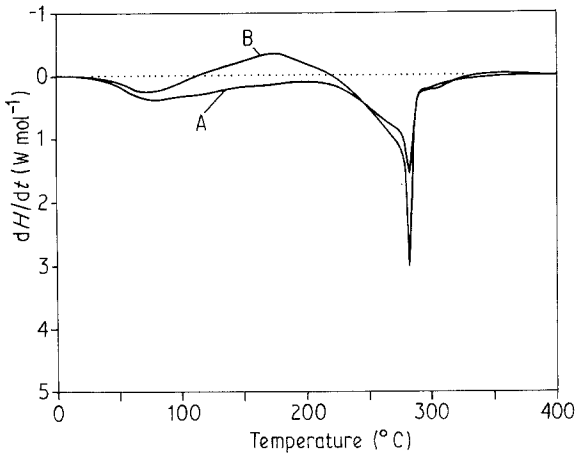

Figure 2 DSC curves of Alloys A and B quenched from 450 °C and aged 7 days at RT, then heated at 5 °C min^{-1}.

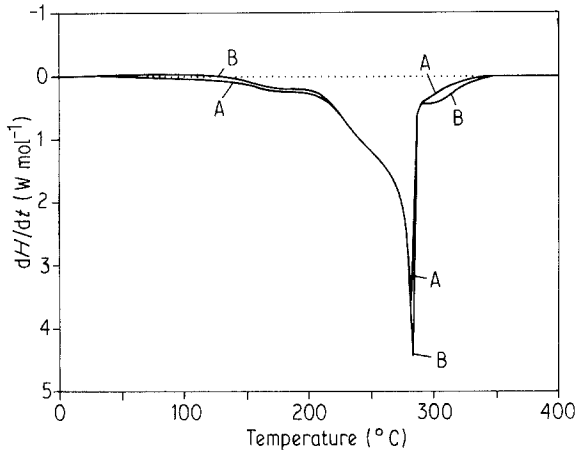

Figure 3 DSC curves of Alloys A and B quenched from 450 °C and aged 7 days at 100 °C, then heated at 5 °C min^{-1}.

contributes to the dissolution effects which follow. Hence the scandium addition does not lead to a substantial decrease in the endothermal effects situated at higher temperatures, contrary to magnesium or copper additions [4].

Ageing for 7 days at 100 °C leads to complete decomposition of the solid solutions according to the hardness tests. The corresponding DSC heating curves in Fig. 3 exhibit essentially endothermal peaks which are slightly more important in Alloy B and much larger than after RT ageing.

In order to identify thermal effects observed in DSC studies with structure changes, transmission electron microscopic observations were performed of samples heated in the same manner. Fig. 4 shows an electron micrograph taken from Alloy B aged 3 days at RT, at

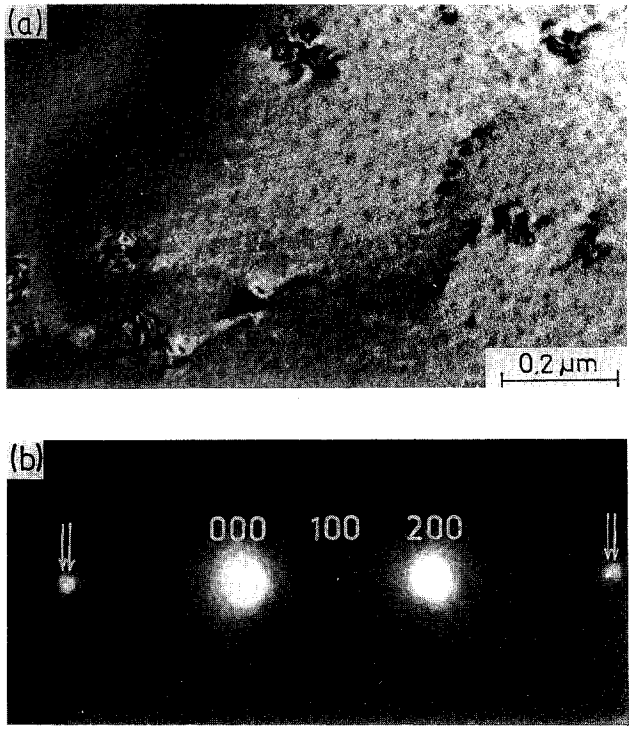

Figure 4 Alloy B aged 3 days at RT. (a) Transmission electron micrograph, (b) 200 row of reflections of selected-area diffraction pattern (SADP).

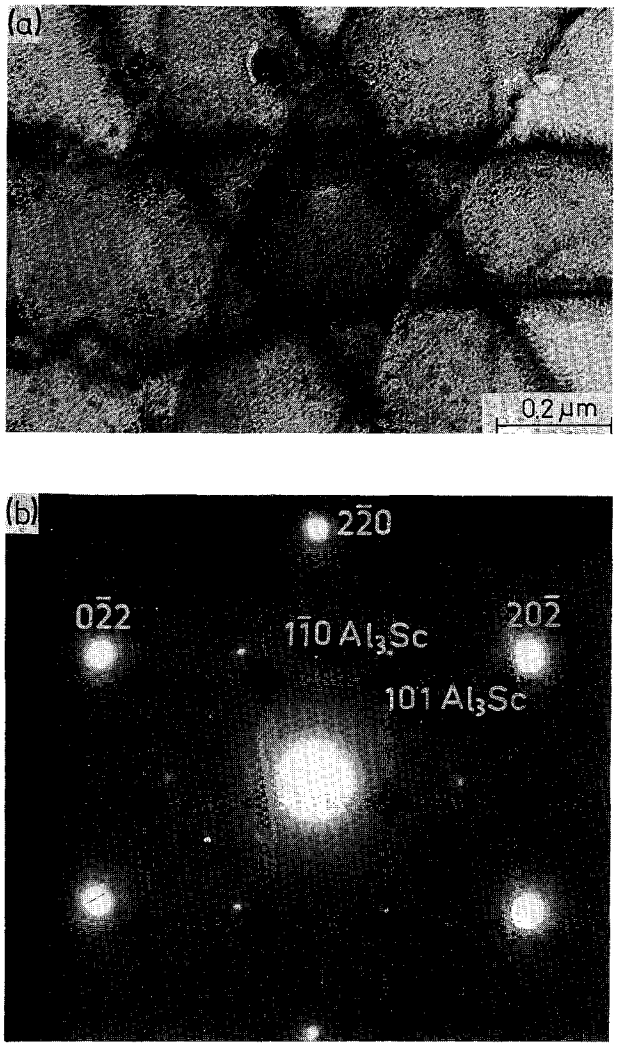

Figure 5 Alloy B quenched and aged at RT for 3 days, then continuously heated to 140 °C at a rate of 5 °C min^{-1}. (a) Transmission electron micrograph, (b) SADP indicating [1 1 1] zone axis orientation.

orientation close to [0 0 1] zone axis and at $g = [2\,0\,0]$ operating. A fine contrast of small dark dots appears due to modulations forming side bands at 200 and 400 reflections (Fig. 4b). The average distance of these modulations is equal to about 4 nm, as judged from the micrograph and the distance of side bands. Additionally, large precipitates accompanied by dislocations can be seen. These are Al_3Sc particles distributed nonhomogeneously within the grains. Weak reflections at 1 0 0 positions appear due to $L1_2$ ordering of Al_3Sc precipitates.

Fig. 5a shows a transmission electron micrograph taken after continuous heating up to 140 °C. It exhibits much coarser modulations of average distance close to 10 nm. Near Al_3Sc precipitates, a darker contrast can be seen, most probably due to β-zinc precipitation. The amount of dark zinc precipitates increases during observation of thin foils in the electron microscope, probably due to a local heating effect. The electron diffraction pattern in Fig. 5b shows symmetrical [1 1 1] zone axis orientation with additional 1 1 0 type reflections of Al_3Sc and 1$\bar{1}$0 0 type zinc reflections. This observation indicates that the exothermal peak observed during continuous heating of Alloy B is most probably due to α'_r and β precipitation which is masked by strong dissolution effects in Alloy A.

The last micrograph (Fig. 6) was taken from Alloy B after heating up to 200 °C, where a dissolution starts, as can be seen in Fig. 2. It shows spherical Al_3Sc precipitates appearing bright in the dark-field micrograph (taken using 1 1 0 Al_3Sc reflection) and elongated α'_r and β particles running in two perpendicular ⟨1 1 0⟩ directions. The nucleation of β precipitates at Al_3Sc particles is clearly visible in this micrograph. The electron diffraction pattern (Fig. 6b) shows significant streaks in ⟨1 1 0⟩ directions due to the presence of α'_r and β precipitates. The splitting of the 1 1 0 Al_3Sc reflection toward the 1 1 0 Al superlattice position is most probably due to zinc dissolution in Al_3Sc particles. It shows a decreasing tendency of the Al_3Sc lattice parameter with zinc dissolution. This would lower the hardening effect due to the presence of Al_3Sc, which is associated with an increased lattice constant as compared to aluminium [8].

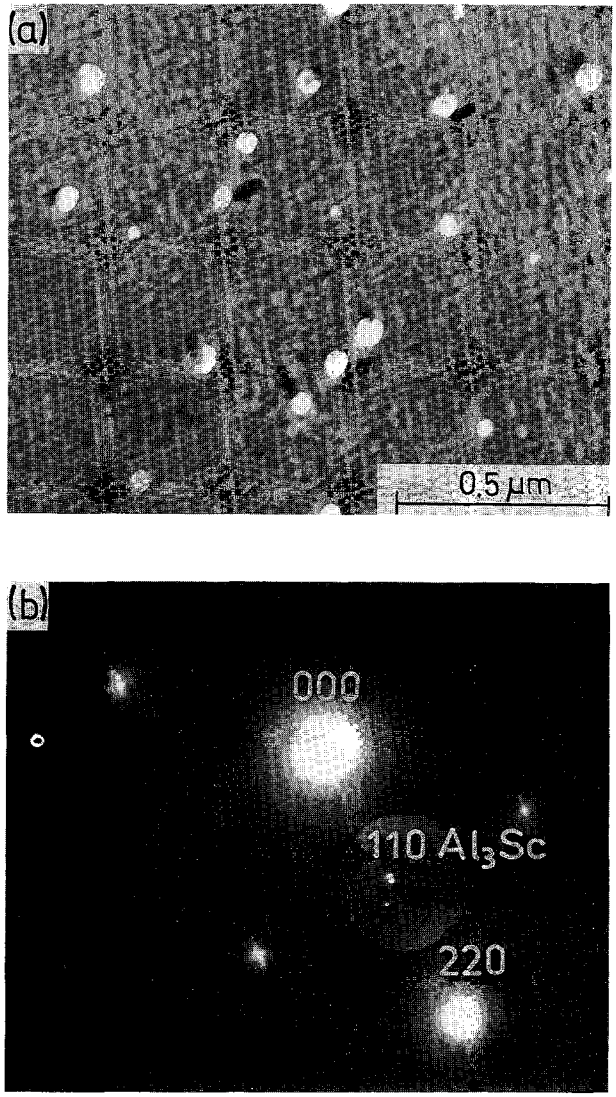

Figure 6 Alloy B quenched and aged at RT for 3 days, then continuously heated to 200 °C at a rate of 5 °C min^{-1}. (a) Dark-field electron micrograph taken using 1 1 0 Al_3Sc spot, (b) SADP showing zone axis orientation close to [0 0 1].

4. Conclusions

1. The addition of scandium does not increase the hardness of aluminium–zinc alloys during ageing, due to insignificant precipitation of finely distributed Al_3Sc particles. Zinc probably dissolves in Al_3Sc thereby decreasing its lattice parameter and consequently the hardening effect.

2. During continuous heating, both alloys show similar heat evolution after RT ageing. At first an endothermal effect accompanies the dissolution of modulations present in quenched and aged alloys. Then an exothermal effect appears in the temperature range 120–200 °C in alloys with scandium addition due to increased heterogeneous precipitation of α'_r and β on large Al_3Sc particles. Heating above 200 °C causes endothermal effects due to dissolution of α'_r and β phases followed by the monotectoid reaction. Decomposition of alloys at 100 °C prior to continuous heating causes significant increases of these latter heat effects.

References

1. M. E. DRITS, L. S. TOROPOVA and J. G. BYKOV, *Metallov. Term. Obr. Met.* **7** (1983) 60.
2. M. E. DRITS, J. DUTKIEWICZ, L. S. TOROPOVA and J. SALAWA, *Cryst. Res. Technol.* **19** (1984) 1325.
3. L. S. TOROPOVA, J. G. BYKOV, V. M. LAZARENKO and J. M. PLATOV, *Fiz. Met. Metallov.* **54** (1982) 201.
4. A. M. ZAHRA, C. Y. ZAHRA, J. DUTKIEWICZ and R. CIACH, *J. Mater. Sci.* **25** (1990) 391.
5. M. SIMERSKA, B. MAJOR, V. SYNECEK, P. BARTUSKA and W. BALIGA, *Arch. Metall.* **32** (1987) 421.
6. R.CIACH, J. DUTKIEWICZ, J. SALAWA and W. BALIGA, *Arch. Hutn.* **19** (1974) 149.
7. R. CIACH, J. DUTKIEWICZ, H. LOEFFLER and G. WENDROCK, in "Proceedings of the Conference on Applied Crystallography" (Silesian University, Katowice, Kozubnik, 1978) p. 728.
8. K. A. GSCHNEIDNER and F. W. CALDERWOOD, *Bull. Alloy Phase Diagrams* **10** (1989) 85.

Received 6 February
and accepted 16 April 1991